

Electronic Supporting Information

Extracting Large photovoltages from a-SiC Photocathodes with an Amorphous TiO₂ Front Surface Field Layer for Solar Hydrogen Evolution

Ibadillah A. Digdaya,^a Lihao Han,^b Thom W. F. Buijs,^b Miro Zeman,^b Bernard Dam,^a Arno H. M. Smets^b and Wilson A. Smith.^{a*}

1 Electrochemical Impedance Spectroscopy

1.1 a-SiC photocathodes

The flat band potential (V_{fb}) and the acceptor concentration (N_A) of the (p/i) a-SiC photocathode was characterized by the electrochemical impedance spectroscopy (EIS) and was estimated using the Mott-Schottky relationship¹:

$$\frac{1}{C_{SC}^2} = \frac{2}{\epsilon_0 \epsilon_r e N_A} \left(V - V_{fb} - \frac{kT}{e} \right) \quad \text{Eq. 1}$$

In this equation, C_{SC} is the space charge capacitance density, ϵ_0 is the vacuum permittivity, ϵ_r is the relative permittivity of a-SiC (14)², e is the electron the charge, A is the active surface area (0.283 cm²), k is the Boltzmann's constant and T is the temperature (298). Figure 1 shows the Mott-Schottky plot of the (p/i) a-SiC at chosen frequency 0.5 kHz.

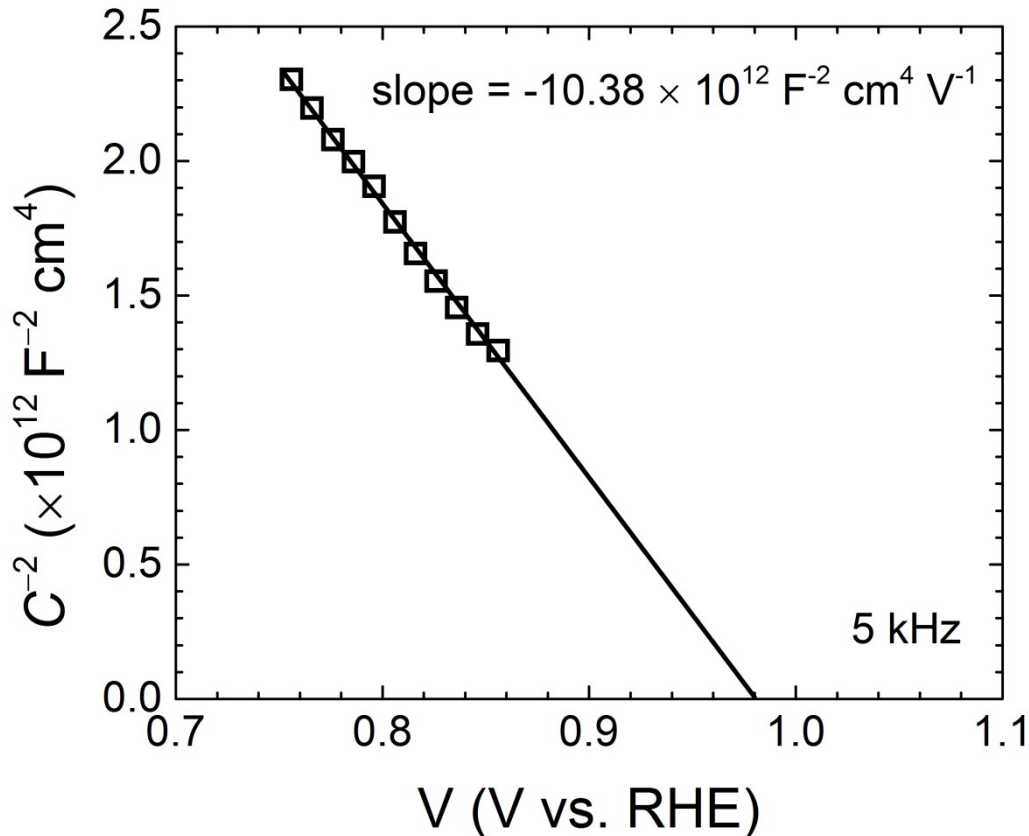


Figure S1 Mott-Schottky plot of the (p/i) a-SiC at 5 kHz taken in the dark.

The V_{fb} can be obtained from intercept between the extrapolated linear line and x-axis of the Mott-Schottky plot, which is estimated to be ~ 0.98 V vs. RHE. Using the Eq. 1 the N_A of the

is approximated to be $9.69 \times 10^{17} \text{ cm}^{-3}$. The valence band edge E_V position can be determined using the following relationship:

$$E_F - E_V = -\frac{kT}{e} \ln\left(\frac{N_A}{N_V}\right) \quad \text{Eq. 2}$$

The density of valance band states (N_V) can be obtained using the following equation:

$$N_V = 2 \left(\frac{2\pi m_h^* kT}{h^2} \right)^{3/2} \quad \text{Eq. 3}$$

where the effective mass of hole (m_h^*) of $0.3m_0$ is assumed to be the same to that c-Si³. Using the above formula, the N_V is calculated to be $4.08 \times 10^{18} \text{ cm}^{-3}$. This suggests that the Fermi level is positioned at 36.94 mV above the valence band edge.

1.2 TiO₂

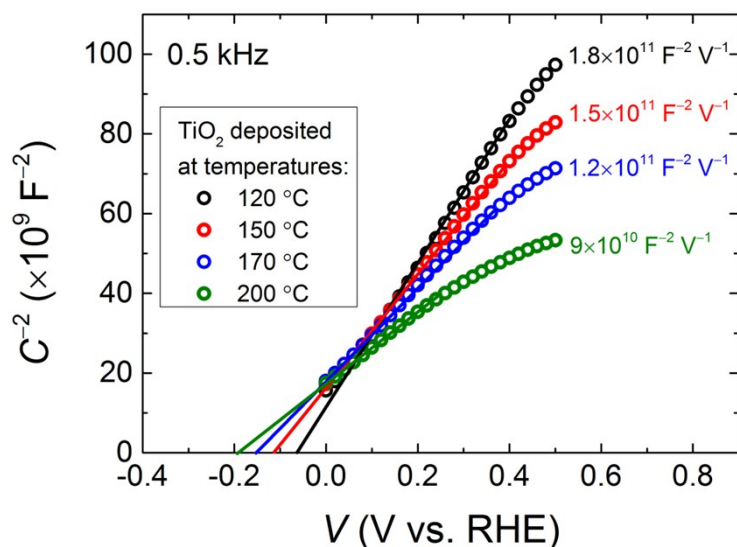


Figure S2 Mott-Schottky plots of TiO₂ films deposited onto FTO glass substrate at various temperatures measured at a frequency of 500 Hz. The intersection of the extrapolated linear line with the x-axis represents the V_{fb} and the difference in slopes reflects the variation in the donor density. All measurements were performed in 0.5 M potassium hydrogen phthalate (pH 4) electrolyte solution.

The donor density (N_D), the effective mass of density of states in the conduction band (N_C) and the position of the Fermi level relative to the conduction band of TiO₂ ($E_{CB}-E_F$) were calculated using the equations in the main paper and are summarized in Table S1.

Table S1 The electronic properties of TiO₂ as obtained from the Mott-Schottky results.

<i>n</i> -type	E_{fb} (V/RHE)	N_C (cm ⁻³)	N_D (cm ⁻³)	$E_{CB}-E_F$ (mV)
TiO ₂ (120 °C)	-0.06	7.86×10^{20}	1.30×10^{20}	46.12
TiO ₂ (150 °C)	-0.11	7.86×10^{20}	1.56×10^{20}	41.44
TiO ₂ (170 °C)	-0.15	7.86×10^{20}	1.96×10^{20}	35.71
TiO ₂ (200 °C)	-0.2	7.86×10^{20}	2.61×10^{20}	28.32

From Table S1, it is apparent that TiO₂ deposited at different temperatures do not show significant variations of V_{fb} and N_D . Seger et al. reported that TiO₂ still allowed effective electron transport in the conduction even with low electron density (10^{17})⁴. Since our ALD TiO₂ already show very high electron density, no further attempt to increase the deposition temperature nor vacuum annealing to improve the conductivity of the film.

2 Optical band gap

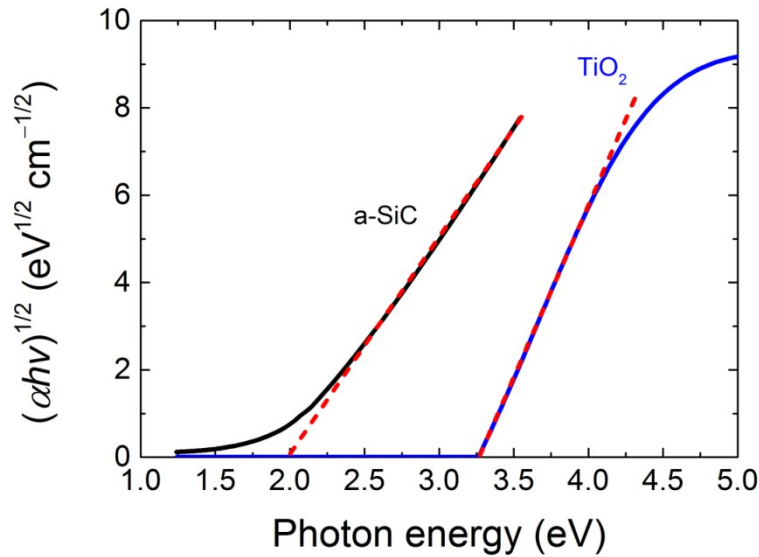


Figure S3 Tauc plot of the a-SiC based on the refractive indices (n & k) measured using the spectroscopy ellipsometry. The interception between the extrapolated linear line and the x-axis represents the direct optical band gap. The band gap of a-SiC and TiO₂ are 2 eV and 3.25 eV, respectively.

3 Solar photocurrent & irradiance spectra

The solar photocurrent is obtained by the multiplication of the IPCE spectrum with the spectral irradiance⁵ of the ASTM AM1.5G⁶ (1000W/m²):

$$I(\lambda) = IPCE \cdot E(\lambda) \cdot \lambda \cdot e/hc$$

Eq. 4

where $I(\lambda)$ is the solar photocurrent spectrum, $E(\lambda)$ is the spectral irradiance of the ASTM AM1.5G, h is the Planck's constant and c is the speed of light in vacuum. The total photocurrent of the photocathode under ASTM AM1.5G illumination is obtained by the integration over the spectrum:

$$j_{ASTM\ AM1.5G} = \int I(\lambda)d(\lambda) \quad \text{Eq. 5}$$

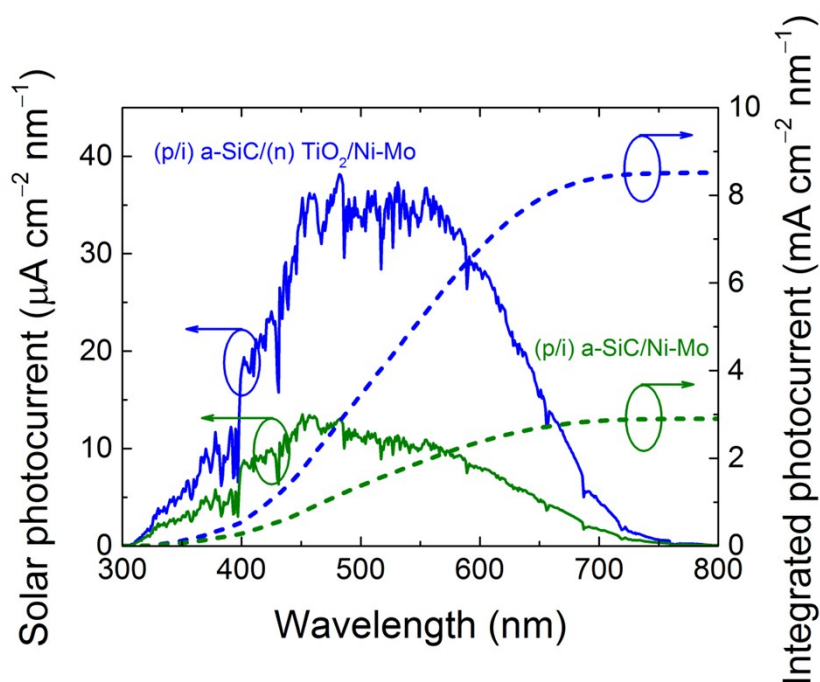


Figure S4 Solar photocurrent spectra of the (p/i) a-SiC (green solid line) and the (p/i) a-SiC/(n) TiO₂ (solid blue line) photocathodes at 0 V vs. RHE and the integrated photocurrent of the corresponding photocathodes (dash lines) at the same wavelengths.

Using Eq. 5 the solar photocurrent of the (p/i) a-SiC and the (p/i) a-SiC/(n) TiO₂ photocathodes can be calculated, that are 1.72 mA cm⁻² and 10.96 mA cm⁻², respectively.

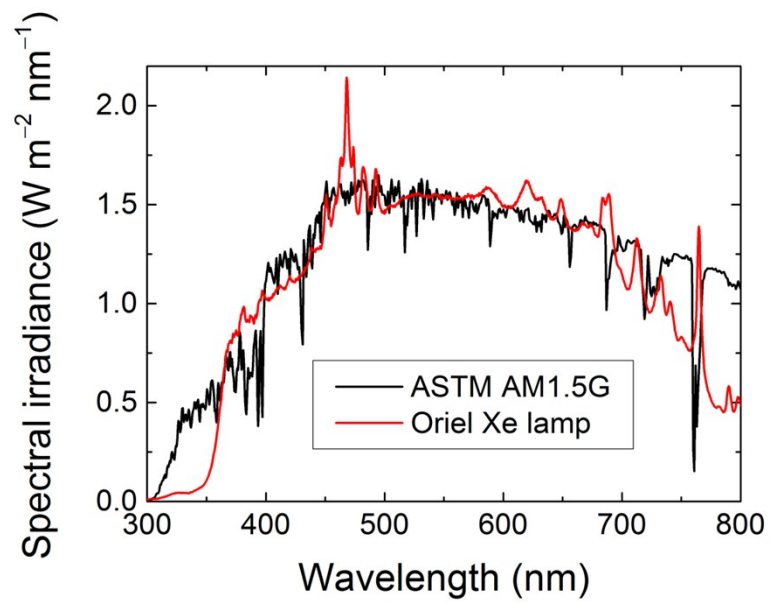


Figure S5 Irradiance spectra of the solar simulator Xe lamp used for j - V measurements (red line) and the ASTM AM1.5G (black line).

4 j - V characteristics

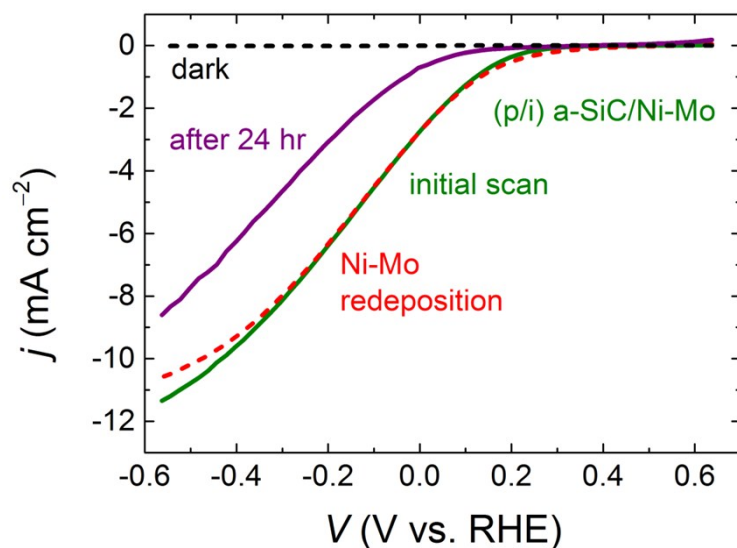


Figure S6 Illuminated j - V characteristics of the Ni-Mo coated (p/i) a-SiC photocathode before (green line) and after stability (purple line) test and after Ni-Mo redeposition (red dash line) measured in a 0.5 M potassium hydrogen phthalate electrolyte at pH 4.

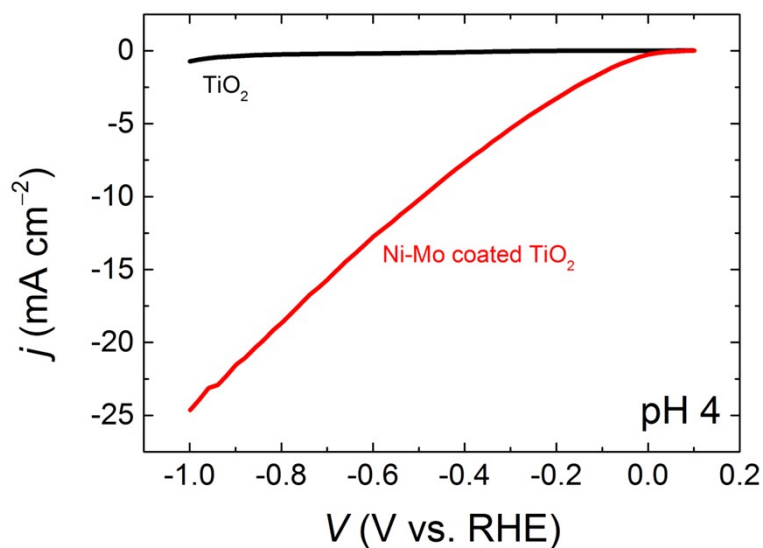


Figure S7 dark j - V characteristics of the FTO coated by TiO_2 and $\text{TiO}_2/\text{Ni-Mo}$ in potassium hydrogen phthalate solution at pH 4. The TiO_2 was deposited at 150 °C. The FTO/Ni-Mo/ TiO_2 shows nearly zero overpotential for hydrogen evolution reaction as indicated by the V_{onset} of 0 V vs. RHE.

5 SEM image and photograph

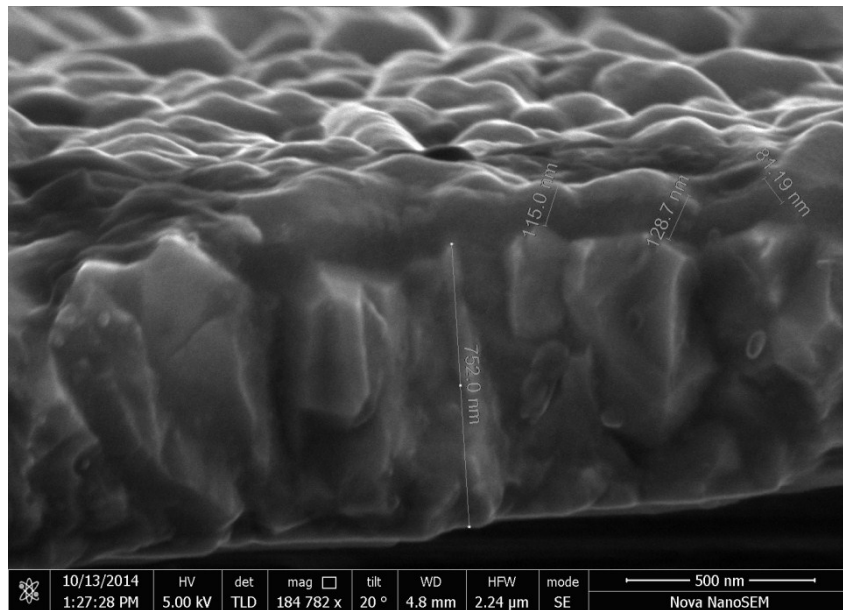


Figure S8 Cross-sectional SEM image of the (p/i) a-SiC/(n) TiO₂, showing the approximate thickness of the film.

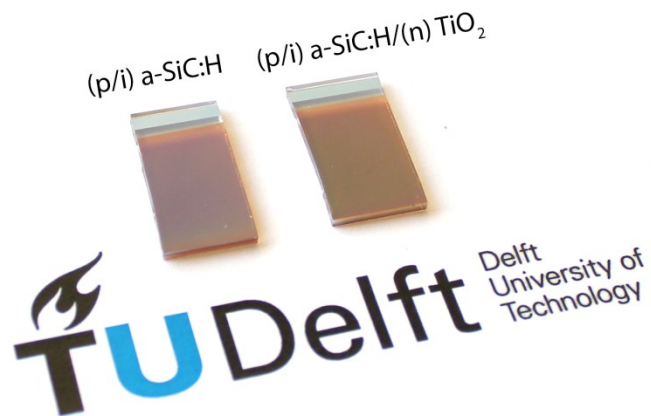
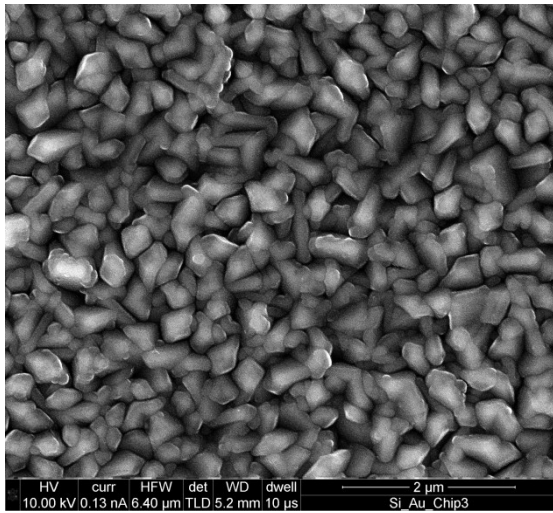
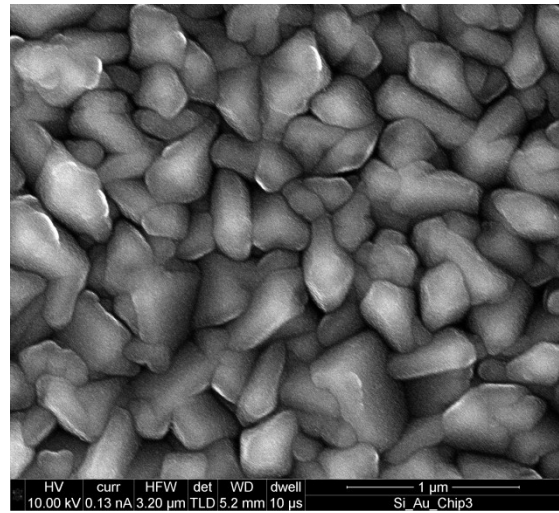


Figure S9 Photograph of the (p/i) a-SiC and the (p/i) a-SiC/(n) TiO₂ samples.

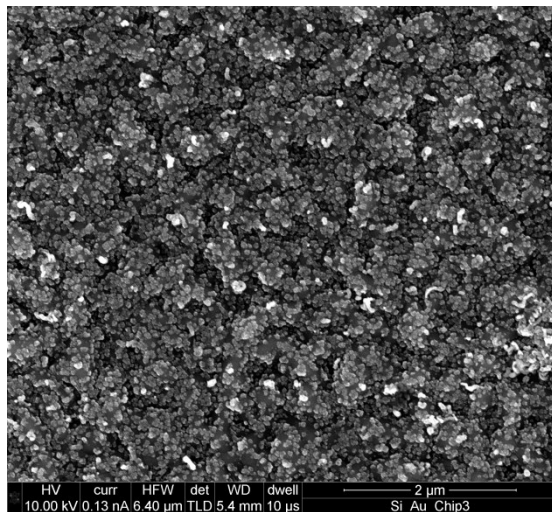


a

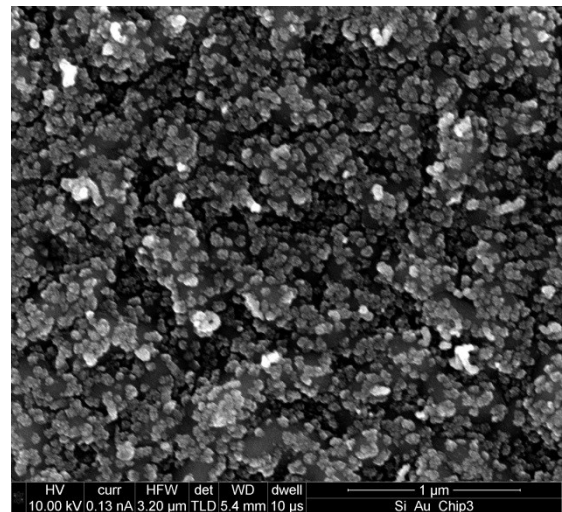


b

Figure S10 a) Top-view SEM image of the (p/i) a-SiC/(n) TiO₂ and b) the magnification of Figure S10a



a



b

Figure S11 a) Top-view SEM image of the (p/i) a-SiC/(n) TiO₂/Ni-Mo and b) the magnification of Figure S11a

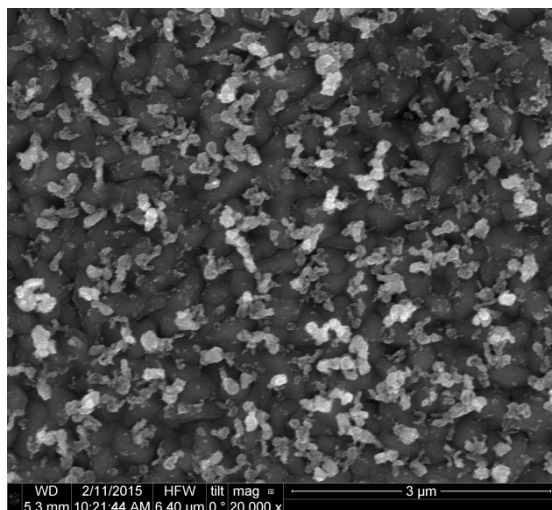


Figure S12 Top-view SEM image of the (p/i) a-SiC/(n) TiO₂/Ni-Mo after chronoamperometry measurement for 12 hours.

References

1. K. Gelderman, L. Lee and S. W. Donne, *Journal of Chemical Education*, 2007, **84**, 685.
2. D. Brassard and M. a. El Khakani, *Journal of Applied Physics*, 2003, **93**, 4066.
3. M. W. M. van Cleef, R. E. I. Schropp and F. a. Rubinelli, *Applied Physics Letters*, 1998, **73**, 2609.
4. B. Seger, T. Pedersen, A. B. Laursen, P. C. K. Vesborg, O. Hansen and I. Chorkendorff, *Journal of the American Chemical Society*, 2013, **135**, 1057–64.
5. A. Kay, I. Cesar and M. Grätzel, *Journal of the American Chemical Society*, 2006, **128**, 15714–21.
6. American Society for Testing and Materials (ASTM), <http://rredc.nrel.gov/solar/spectra/am1.5/>.